Sterol Carrier Protein-2-Facilitated Intermembrane Transfer of Cholesterol- and Phospholipid-Derived Hydroperoxides†

Andrew Vila,‡ Vladislav V. Levchenko,‡ Witold Korytowski,‡§ and Albert W. Girotti*,‡

Department of Biochemistry, Medical College of Wisconsin, Milwaukee, Wisconsin 53226, and Institute of Molecular Biology, Jagiellonian University, Krakow, Poland

Received April 30, 2004; Revised Manuscript Received August 3, 2004

ABSTRACT: Sterol carrier protein-2 (SCP-2) facilitates cholesterol (Ch) and phospholipid (PL) transfer/exchange between membranes and appears to play a key role in intracellular lipid trafficking. Whether SCP-2 can also facilitate lipid hydroperoxide (LOOH) transfer between membranes and thereby potentially enhance dissemination of peroxidative damage was examined in this study. Transfer kinetics of photochemically generated cholesterol hydroperoxide (ChOOH) species (5α-OOH, 6α/6*β*-OOH, 7α/7*β*-OOH) and phospholipid hydroperoxide (PLOOH) families (PCOOH, PEOOH, PSOOH) were determined, using HPLC with electrochemical detection for peroxide analysis. LOOH donor/acceptor pairs employed in transfer experiments included (i) all liposomes (e.g., agglutinable SUVs/ nonagglutinable LUVs); (ii) photoperoxidized erythrocyte ghosts/SUVs or vice versa; and (iii) SUVs/mitochondria. In a SUV/ghost system at 37 °C, the rate constant for total ChOOH spontaneous transfer was ∼8 times greater than that for unoxidized Ch. Purified bovine liver and human recombinant SCP-2 exhibited an identical ability to stimulate overall ChOOH transfer, 0.5 unit/mL (based on [^{14}C]Ch transfer) increasing the first-order rate constant (*k*) ∼7-fold. SCP-2-enhanced translocation of individual ChOOHs increased with increasing hydrophilicity in the following order: 6*β*-OOH < 6α-OOH < 5α-OOH < 7α/7*β*-OOH. Likewise, SCP-2 stimulated PCOOH, PEOOH, or PSOOH transfer ∼6-fold, but the net *k* was 1/5 that of 5α-OOH and 1/10 that of 7α/7*β*-OOH. Donor membrane properties favoring SCP-2-enhanced LOOH transfer included (i) increasing PL unsaturation and (ii) increasing net negative charge imposed by phosphatidylserine. Cytotoxic relevance was demonstrated by showing that SCP-2 accelerates 7α-OOH transfer from SUVs to isolated mitochondria and that this enhances peroxide-induced loss of the mitochondrial membrane potential. On the basis of these findings, we postulate that SCP-2, by trafficking ChOOHs and PLOOHs in addition to parent lipids, might exacerbate cell injury under oxidative stress conditions.

Unsaturated lipids in membrane compartments of mammalian cells are susceptible to enzymatic and nonenzymatic peroxidation, a process that can have normophysiologic as well as pathophysiologic consequences (*1*, *2*). Lipid hydroperoxides (LOOHs),[1] including phospholipid (PL)- and cholesterol (Ch)-derived species, are important nonradical products/intermediates in these reactions (*3*). Enzymatic lipid peroxidation is typically catalyzed by cyclooxygenases or lipoxygenases and generates specific LOOHs in relatively small numbers (*4*). In contrast, nonenzymatic lipid peroxidation induced by reactive oxygen species such as hydroxyl radical (HO$^{\bullet}$) and singlet oxygen ($^1O_2$) or by reactive nitrogen oxide species such as peroxynitrite ($ONOO^-$) and nitrogen dioxide ($^{\bullet}NO_2$), typically produces a broader spectrum of LOOHs along with other compounds and is not subject to cellular regulation (*2*, *3*). Once formed, LOOHs can have a variety of fates that may impact on the metabolic status and viability of a targeted cell. For example, a nascent LOOH may undergo iron-catalyzed one-electron reduction to free radical species which trigger damaging (toxicity-enhancing) chain peroxidation reactions (*3*). Alternatively, selenoper-

† This work was supported by USPHS Grants CA72630 and TW01386 (A.W.G.), KBN Grant 3P05A-5523 (W.K.), and NRSA Predoctoral Fellowship F31-CA85171 (A.V.).

* To whom correspondence should be addressed. Tel: (414) 456-8432; fax: (414) 456-6510; e-mail: agirotti@mcw.edu.

‡ Medical College of Wisconsin.

§ Jagiellonian University.

[1] Abbreviations: $AlPcS_2$, aluminum phthalocyanine disulfonate; Ch, cholesterol; ChOOH(s), cholesterol hydroperoxide(s); BHT, butylated hydroxytoluene; BSA, bovine serum albumin; DFO, desferrioxamine; DCP, dicetyl phosphate; DMPC, 1,2-dimyristoyl-*sn*-glycero-3-phosphocholine; DTT, dithiothreitol; DTNB, 5,5′-dithiobis (2-nitrobenzoate); $Fe(HQ)_3$, ferric 8-hydroxyquinoline, HEPES, *N*-2-hydroxyethylpiperazine-*N*-2-ethanesulfonic acid; HPLC-EC(Hg), high-performance liquid chromatography with mercury cathode electrochemical detection; HPTLC-PI, high-performance thin-layer chromatography with phosphorimaging detection; LacPE, 1,2-dioleoyl-*sn*-glycero-3-phosphoethanolamine-*N*-lactosyl; LOOH(s), lipid hydroperoxide(s); LUV(s), large unilamellar vesicle(s); MOPS, 3-(*N*-morpholino)propanesulfonic acid; MS, Chelex-treated 0.2 M mannitol/50 mM sucrose/5 mM KH_2PO_4/5 mM MOPS (pH 7.2); PBS, Chelex-treated phosphate buffered saline (125 mM NaCl, 25 mM sodium phosphate, pH 7.4); PBS/DFO/EDTA, Chelex-treated PBS containing 0.1 mM DFO and 0.1 mM EDTA.; PL(s), phospholipid(s); PC, phosphatidylcholine; POPC, 1-palmitoyl-2-oleoyl-*sn*-glycero-3-phosphocholine; POPE, 1-palmitoyl-2-oleoyl-*sn*-glycero-3-phosphoethanolamine; POPS, 1-palmitoyl-2-oleoyl-*sn*-glycero-3-phosphoserine; PCOOH, phosphatidylcholilne hydroperoxide; PEOOH, phosphatidylethanolamine hydroperoxide; PSOOH, phosphatidylserine hydroperoxide; PLOOH(s), phospholipid hydroperoxide(s); Rh123, rhodamine 123; SMOOH, sphingomyelin hydroperoxide; SUV(s), small unilamellar vesicle(s); 5α-OOH, 3*β*-hydroxy-5α-cholest-6-ene-5-hydroperoxide; 6α-OOH, 3*β*-hydroxycholest-4-ene-6α-hydroperoxide; 6*β*-OOH, 3*β*-hydroxycholest-4-ene-6*β*-hydroperoxide; 7α-OOH, 3*β*-hydroxycholest-5-ene-7α-hydroperoxide; 7*β*-OOH, 3*β*-hydroxycholest-5-ene-7*β*-hydroperoxide; 7α/7*β*-OOH, undefined mixture of 7α-OOH and 7*β*-OOH; 7α-OH, cholest-5-ene-3*β*,7α-diol.

10.1021/bi0491200 CCC: $27.50 © 2004 American Chemical Society
Published on Web 09/09/2004

oxidase-catalyzed detoxification of LOOHs may occur (i.e., GSH-dependent two-electron reduction to relatively innocuous alcohols (LOHs) (*3*)). Enzymatic transesterification could provide an additional pathway for detoxification; for example, lecithin-Ch acyltransferase might transfer a peroxidized fatty acyl group from a PLOOH to Ch, giving a cholesteryl ester hydroperoxide, which is sequestered and subsequently two-electron reduced (*5*, *6*). The degree of partitioning between the one- and two-electron pathways could ultimately determine how a cell responds to a LOOH challenge. We recently recognized that these reactions are not necessarily limited to the membrane where LOOHs originate, as widely assumed, but can extend to other membranes via a translocation process (*7*−*9*). Being more hydrophilic than parent lipids, LOOHs would move more readily into the aqueous compartment, thus increasing the probability of transfer. Using photoperoxidized erythrocyte ghosts as donors and small liposomes (SUVs) as acceptors at 37 °C, we showed that cholesterol hydroperoxides (ChOOHs) as a group translocate spontaneously and reversibly with a rate constant ~65-times greater than that of parent Ch (*8*). As in the case of Ch itself (*10*), spontaneous ChOOH transfer occurs via an aqueous transit pool rather than membrane collision, the rate-limiting step being desorption from the donor membrane (*7*, *8*). For individual ChOOH species separated by reverse phase HPLC, striking differences in transfer kinetics were observed, the rank order being identical to that for hydrophilicity (i.e., 7α/7*β*-OOH > 5α-OOH > 6α-OOH > 6*β*-OOH). The same trend has been observed with a variety of donor/acceptor transfer models, including ghosts/SUVs (*7*, *8*), ghosts/low-density lipoprotein (*9*), and SUVs/tumor cells (*8*). Similarly, the ability of phospholipid hydroperoxide (PLOOH) families to translocate, and at substantially greater rates than parent PLs, has been demonstrated (*9*).

Sterol carrier protein-2 (SCP-2), also known as nonspecific lipid transfer protein, is a relatively small (13.2 kDa) intracellular mediator of Ch, PL, and fatty acid trafficking (*11*−*13*). In this study, we have determined that natural bovine or recombinant human SCP-2 can also facilitate the intermembrane movement of ChOOHs and PLOOHs, and that this can exacerbate peroxidative injury at the acceptor site. This is the first reported example of such action by a cellular transfer protein.

MATERIALS AND METHODS

General Materials. 1,2-Dimyristoyl-*sn*-glycero-3-phosphocholine (DMPC), 1-palmitoyl-2-oleoyl-*sn*-glycero-3-phosphocholine (POPC), 1-palmitoyl-2-oleoyl-*sn*-phosphoethanolamine (POPE), 1-palmitoyl-2-oleoyl-*sn*-glycero-3-phospho-l-serine (POPS), egg yolk phosphatidylcholine, and 1,2-dioleoyl-*sn*-glycero-3-phosphoethanolamine-*N*-lactosyl (LacPE) were obtained from Avanti Polar Lipids (Birmingham, AL). Sigma Chemical Co (St. Louis, MO) supplied the antimycin A, butylated hydroxytoluene (BHT), nonradioactive Ch, Chelex-100 (50−100 mesh), carbonyl cyanide *m*-chlorophenylhydrazone (CCCP), desferrioxamine (DFO), dicetyl phosphate (DCP), 5,5′-dithiobis (2-nitrobenzoate) (DTNB), dithiothreitol (DTT), fatty acid-free bovine serum albumin (BSA), 3-morpholinopropanesulfonic acid (MOPS), rotenone, succinic acid, and *Ricinus communis* agglutinin (RCA_{120} or RCA-I). Aluminum phthalocyaninedisulfonate ($AlPcS_2$), an amphiphilic photosensitizing dye, was obtained from Dr. J. Van Lier (University of Sherbrooke) as a gift. A stock solution of $AlPcS_2$ (2.0 mM in dimethyl sulfoxide) was stored in the dark at 4 °C and used indefinitely. Stock ferric 8-hydroxyquinoline [$Fe(HQ)_3$, 1.0 mM in 1 mM HCl/50% ethanol] was prepared as described (*14*). Rhodamine 123 (Rh123) was obtained from Molecular Probes (Eugene, OR) and the Bradford reagent from Bio-Rad (Hercules, CA). Amersham Life Sciences (Arlington Heights, IL) supplied the [4-^{14}C]Ch (~50 mCi/mL), 1-palmitoyl-2-[1-^{14}C]oleoyl-*sn*-3-phosphocholine (~55 mCi/mL), and glycerol tri-[9,10-^{3}H]oleate (~60 mCi/mL), which were HPLC-purified immediately before use (*8*, *9*). HPLC-grade solvents were from Burdick and Jackson Corp. (Muskegon, MI). Nonradioactive ChOOH standards, including singlet oxygen-generated 5α-OOH, 6α-OOH, and 6*β*-OOH and free radical-generated 7α-OOH and 7*β*-OOH were prepared by photoperoxidation of Ch and characterized as described (*15*, *16*). [^{14}C]7α-OOH was prepared similarly using [^{14}C]Ch, and [^{14}C]7α-OH was obtained by triphenylphosphine reduction of the hydroperoxide (*15*). PLOOH standards, including hydroperoxides of POPC, POPE, and POPS, were prepared by photooxidation of the respective PLs in liposomal form and isolated as described (*9*). All peroxide standards were determined iodometrically (*17*) and stored in 2-propanol at −20 °C.

Liposome Preparation. Unilamellar liposomes were fabricated by an extrusion process (*16*, *18*), using an extrusion device from Lipex Biomembranes (Vancouver, BC). Small vesicles (50 nm SUVs) typically served as LOOH donors, whereas large vesicles (200 nm LUVs) were used as acceptors. Typical lipid compositions and bulk phase concentrations of stock SUV suspensions were as follows: (a) 1.0 mM egg PC/0.8 mM [^{14}C]Ch (1.0 μCi/mL)/0.02 mM DCP (for studying Ch and ChOOH transfer from photooxidized SUVs to ghosts); (b) 10 mM DMPC/0.1 mM DCP (for studying ChOOH and PLOOH transfer from photooxidized ghosts); (c) {1.0 mM DMPC, POPC, or egg PC}/0.63 mM Ch/0.16 mM 7α-OOH/0.02 mM DCP (for studying the effect of increasing PL unsaturation on ChOOH transfer); (d) {0.83 mM DMPC, POPC, or egg PC}/0.16 mM POPC-OOH/0.79 mM Ch/0.02 mM DCP (for studying the effect of increasing PL unsaturation on PLOOH transfer); (e) egg PC/{7α-OOH or POPC-OOH}/DCP, where [DCP] was 0.01 mM, [egg PC] varied from 0.98 to 0.84 mM, and [7α-OOH] or [POPC-OOH] varied reciprocally from 0.01 to 0.15 mM (for studying LOOH transfer rate in relation to LOOH concentration); (f) 1.0 mM egg PC/0.63 mM Ch/0.16 mM 7α-OOH/0.02 mM DCP or 0.83 mM egg PC/0.16 mM POPC-OOH/0.79 mM Ch/0.02 mM DCP (for studying LOOH transfer kinetics in relation to SCP-2 concentration); (g) POPC/POPS/{1.0 mM 7α-OOH, POPC-OOH, or [^{14}C]-Ch}/1.0 mM LacPE, where [POPC] varied from 8.0 to 5.0 mM, and [POPS] varied reciprocally from 0 to 3.0 mM (for studying ChOOH, POPC-OOH, and Ch transfer kinetics in relation to SUV negative charge); acceptor membranes in this case were from a stock 9.5 mM POPC/0.5 mM POPS LUV preparation; and (h) 0.79 mM POPC/{0.20 mM [^{14}C]7α-OOH or [^{14}C]7α-OH (20 nCi/mL)}/0.01 mM DCP (for studying the damaging effects of 7α-OOH vs 7α-OH transfer to mitochondria). The net negative charge imposed by DCP (~1 mol %) inhibited any membrane fusion and fostered SCP-2 binding. The aqueous phase for all liposome

preparations was PBS that had been Chelex-treated to remove metal ions that might otherwise catalyze LOOH turnover or generation. Stock suspensions were stored under argon at 4 °C and used experimentally within 3−4 days.

Erythrocyte Ghost Preparation. Human erythrocyte ghosts were prepared as described (*9*) and stored in PBS/DFO/EDTA under argon at 4 °C. Total membrane protein was determined by Bradford assay (*19*), and total lipid molar concentration was calculated from the known lipid/protein mass ratio and overall lipid composition (wt %) (*20*). For measuring transfer of unoxidized Ch and PC, ghosts were labeled with [^{14}C]Ch and [^{14}C]POPC simultaneously, as described (*9*). Any lipid autoxidation during labeling incubation was negligible.

Preparation of Mitochondria. Mouse liver mitochondria were prepared by differential centrifugation (*21*) and further purified on a sucrose gradient, as described (*22*). The recovered mitochondrial fraction was washed with and resuspended in isolation buffer (*22*) lacking EGTA. Protein concentration was determined by Bradford assay (*19*), and molar concentration of total lipid was calculated using the known protein/lipid mass ratio and the overall lipid composition (wt %) (*23*). Mitochondria were used experimentally within 2 h after preparation.

Preparation and Characterization of SCP-2. Bovine liver SCP-2 was prepared as described (*24*), with slight modification (K. W. A. Wirtz, personal communication). Upon SDS−PAGE analysis, the isolated protein appeared as a single band with M_r ∼13 kDa, in agreement with reported values for SCP-2 (*12*, *13*). Amino acid analysis carried out at the Protein/Nucleic Acid Core Facility at this institution revealed the following N-terminal sequence: SSSVDGFKANLVFK-EIEKKL, which is identical to the known sequence for bovine SCP-2 (*25*). Incubation of a dialyzed protein sample with a 10-fold molar excess of Ellman's reagent (DTNB) for 30 min in PBS at 37 °C, followed by A_{412} measurement (*26*), revealed a cysteine thiol content of 0.95 ± 0.05 mol/mol of protein, in agreement with a published value (*25*). Concurrent with thiol oxidation by DTNB, there was a >90% loss of [^{14}C]Ch transfer activity, consistent with earlier evidence (*26*); both effects were substantially (>70%) reversed by incubation with 1 mM DTT for 30 min. The purified bovine protein, quantified by Bradford assay (*19*), was stored at −20 °C in 10 mM potassium phosphate buffer (pH 6.8) containing 0.1 mM DFO, 5 mM DTT, and 50% glycerol.

Recombinant SCP-2 was prepared as described previously (*27*), using an *Escherichia coli* strain bearing a plasmid encoded for the 13.2 kDa human protein (kindly provided by F. Schroeder, Texas A&M University). The purified protein was stored at −20 °C in 10 mM potassium phosphate (pH 6.8)/0.5 mM EDTA/1 mM DTT/50% glycerol. Immediately before being used in transfer experiments, stock SCP-2 solutions were dialyzed against PBS/DFO/EDTA at 4 °C to remove interfering DTT and glycerol.

SCP-2 specific activity was assessed in terms of enhanced [^{14}C]Ch transfer from eggPC/[^{14}C]Ch/DCP (5:4:0.1 by mol) SUVs to ghost acceptors in 10-fold lipid molar excess. Incubation in PBS/DFO/EDTA at 37 °C was carried out in the absence and presence of SCP-2 (typically ∼25 μg/mL). Samples were recovered periodically over a 1 h period and centrifuged, and residual [^{14}C]Ch in the supernatant (SUV) fraction was determined by scintillation counting. Initial transfer rates were calculated from first order decay data, total minus background rate giving the net SCP-2-enhanced rate. One unit of activity is defined as the amount of protein translocating 1 nmol of Ch per min. Stock preparations of bovine and human recombinant SCP-2 typically exhibited specific activities of 5−10 units/mg of protein and 20−25 units/mg of protein, respectively.

Membrane Photoperoxidation. Erythrocyte ghosts or egg PC/[^{14}C]Ch/DCP SUVs were subjected to $^1O_2$-mediated photoperoxidation using $AlPcS_2$ as a sensitizer (*17*). Ghost membranes [1.0 mg of protein/mL (0.56 mM Ch and 0.67 mM PL in bulk suspension)] were sensitized with 20 μM $AlPcS_2$, transferred to a thermostated beaker at 25 °C, and irradiated from above, using a quartz-halogen light source (fluence rate ∼150 mW/cm^2) and gentle magnetic stirring. SUVs were photoperoxidized similarly at 4 °C. ChOOHs and PLOOHs accumulated linearly with increasing light fluence in both membrane systems, the respective rates for ghosts being ∼2 and ∼8 μM/min. Thus, 20 min of irradiation produced ∼40 μM total ChOOH (7% of starting Ch) and ∼160 μM total PLOOH (24% of starting PL) in ghost suspensions. HPLC-EC(Hg) analysis indicated that the ChOOH was typically apportioned as ∼70% 5α-OOH, 10% 6α-OOH, 15% 6β-OOH, and 5% 7α/7β-OOH, while the PLOOH was apportioned as ∼45% PCOOH, 41% PEOOH, and 10% PSOOH, SMOOH (∼4%) being barely resolved from PCOOH. Peroxidized ghosts were washed twice with PBS/DFO to remove any fragmented membranes and used immediately in transfer experiments.

Experimental Transfer Conditions. SCP-2-enhanced translocation of Ch and ChOOH was examined initially, using photoperoxidized SUVs as donors and erythrocyte ghosts as acceptors. Transfer incubation was carried out in the dark to avoid any further photoperoxidation by SUV-associated $AlPcS_2$. A typical reaction mixture (2.0 mL) contained peroxidized egg PC/[^{14}C]Ch/DCP (50:40:1 by mol) SUVs (0.06 mM total lipid; ∼23 μM Ch and 4 μM ChOOH), unoxidized ghost membranes (0.6 mM total lipid), bovine or human recombinant SCP-2 (∼0.5 unit/ mL), and BHT (10 μM) in PBS/DFO/EDTA at 37 °C. A mixture containing everything except SCP-2 was prepared alongside for assessing background (spontaneous) translocation. BHT, a chain-breaking antioxidant (*1*, *2*), was included with DFO and EDTA to further reduce the possibility of new LOOH formation during transfer incubation; neither BHT nor its ethanol vehicle had any significant effect on transfer kinetics (*8*). Reactions were carried out in 10 mL Pyrex tubes inserted into a thermal block and capped with glass marbles. At various time points up to 2 h, a 0.1 mL aliquot from each mixture was transferred to a microfuge tube, diluted with an equal volume of ice-cold PBS to quench transfer (*7*), and centrifuged at 4 °C. A 0.1 mL aliquot of the SUV-containing supernatant was adjusted to 0.25 mL with PBS/1 mM EDTA and extracted with 0.4 mL of chloroform/methanol (2:1 by vol) (*17*). For determining ChOOH or Ch in the entire system, matching samples were extracted without centrifugation−separation of the membrane components (typically at the beginning, middle, and end of an incubation). A 0.2 mL aliquot from each organic phase was dried under N_2, and recovered material was stored at −20 °C prior to analysis of [^{14}C]Ch and [^{14}C]ChOOH by HPTLC-PI. Since individual ChOOH isomers are not well-resolved by HPTLC (*7*, *8*),

translocated material measured by this approach represented the overall ChOOH population. Ghost membranes were also used as acceptors in experiments that examined Ch and ChOOH or PL and PLOOH transfer as a function of SCP-2 concentration, SUV hydroperoxide concentration, or degree of SUV PL unsaturation. General reaction conditions were similar to those described previously for a single starting concentration of SCP-2 and ChOOH or Ch.

The ability of SCP-2 to facilitate LOOH transfer was also studied using photoperoxidized ghosts as donors and SUVs as acceptors. A typical reaction mixture contained peroxidized ghosts (0.25 mM lipid), DMPC/DCP (100:1 by mol) SUVs (2.5 mM lipid), 10 μM BHT, and recombinant SCP-2 [$\sim$1 unit (50 μg)/mL] in PBS/DFO/EDTA. For measurement of spontaneous transfer, SCP-2 was omitted. Periodically during incubation at 37 °C, aliquots were removed, quenched with cold PBS, and centrifuged at 4 °C. Recovered ghost pellets were washed at least twice with PBS to remove residual SUVs, resuspended to 0.25 mL with PBS/1 mM EDTA, and extracted with 0.4 mL of chloroform/methanol (2:1 by vol). Other details were as described previously for SUV donors. Recovered lipid fractions were analyzed for remaining ChOOHs or PLOOHs by means of HPLC-EC(Hg). In this case, individual ChOOH species (5α-OOH, 6α-OOH, 6β-OOH, 7α/7β-OOH) or PLOOH families (PCOOH, PEOOH, PSOOH) were separated and determined.

A SUV donor/LUV acceptor system was adopted for studying the effect of negative charge density on SCP-2-mediated 7α-OOH transfer. Separation of SUVs from LUVs during transfer incubation was accomplished using a SUV-specific agglutination procedure (*28*). Incubation mixtures typically contained POPC/POPS/ 7α-OOH/LacPE (865:063:1:1 by mol) SUVs (0.06 mM lipid), POPC/POPS (19:1 by mol) LUVs (0.6 mM lipid), 10 μM BHT, and human recombinant SCP-2 (20 μg/ mL; omitted for assessing spontaneous transfer) in PBS/DFO/EDTA at 20 °C. Reactions were carried out at 20 °C instead of 37 °C to slow facilitated 7α-OOH transfer from negatively charged SUVs and to allow initial rates to be measured more accurately. At various time points during incubation, the reaction was quenched in a microfuge tube by mixing a 25 μL sample with 50 μg of RCA_{120} agglutinin in 100 μL of ice-cold PBS/DFO/EDTA. After a 10 min incubation on ice to allow agglutination of donor vesicles (interaction of RCA_{120} and LacPE), the mixture was centrifuged (16 000*g*, 10 min). A 62.5 μL aliquot of the LUV-containing supernatant was brought to 0.25 mL with cold PBS/1 mM EDTA and extracted; 7α-OOH in the lipid fraction was determined by HPLC-EC(Hg). Effects of negative charge density on SCP-2-mediated Ch transfer were studied similarly, using SUVs that were identical to those described except for the substitution of [^{14}C]Ch for 7α-OOH. Preliminary experiments with LUV acceptors labeled with [^{3}H]triolein ($\sim$2 nCi/mL), a nontransferrable lipid (*29*), revealed that acceptor recovery following RCA_{120} treatment was at least 95%, as determined by scintillation counting. Correspondingly, when SUVs and LUVs were added to RCA_{120} immediately after mixing, <2% of the [^{14}C]Ch or 7α-OOH signal was detected in the LUV compartment. Thus, there was minimal cross-contamination between compartments, confirming the validity of this approach (*28*).

For studying SCP-2-mediated peroxide transfer to mitochondria and its damaging consequences, the reaction system consisted of POPC/[^{14}C]7α-OOH/ DCP (80:20:1 by mol) SUV donors (0.06 mM total lipid), freshly isolated liver mitochondria ($\sim$0.6 mM total lipid), and recombinant SCP-2 (50 μg/mL; omitted for spontaneous transfer measurement) in MS buffer [Chelex-treated 200 mM mannitol/50 mM sucrose/5 mM KH_2PO_4/5 mM MOPS (pH 7.2)]. A control system using [^{14}C]7α-OH instead of [^{14}C]7α-OOH in donor SUVs was set up similarly. Timed samples recovered during transfer incubation 37 °C were centrifuged at 16 000*g* for 1 min to pellet mitochondria. After washing with cold PBS, the mitochondria were resuspended in cold PBS/1 mM EDTA and extracted. Recovered lipid fractions were analyzed for acquired [^{14}C]7α-OOH or [^{14}C]7α-OH by HPTLC-PI. Since 7α-OOH is well-resolved from any 7α-OH or 7β-OH generated by reductive turnover (*7*−*9*), it was possible to visualize not only the extent to which this might have occurred during transfer but also to correct for it in determining 7α-OOH uptake kinetics.

Measurement of Mitochondrial Membrane Potential. Rh123-based fluorometric determination of transmembrane potential ($\Delta\Psi$) was carried out by an established procedure (*30*), with slight modification. The approach is based on membrane potential-driven accumulation of cationic Rh123 by mitochondria. Concomitantly, the dye's fluorescence is quenched so that an inverse relationship exists between measured fluorescence intensity and membrane potential. A QM-7SE scanning spectrofluorometer (Photon Technology International, Ontario, Canada) operating in the photon counting mode was used for fluorescence detection. Excitation was set at 503 nm and emission at 527 nm, using 1 nm slits. Measurements were carried out at 37 °C in a thermostated fluorescence cuvette containing 5 mM sodium succinate, 1 μM rotenone, and 0.2 μM Rh123 in 2.5 mL of $\Delta\Psi$ assay buffer (150 mM sucrose, 20 mM HEPES, 10 mM K_2HPO_4, 5 mM $MgCl_2$; pH 7.4). Transfer-incubated mitochondria were rapidly pelleted, washed, and added to the assay medium, giving a protein concentration of $\sim$0.2 mg/mL. The ensuing decay (quenching) of Rh123 fluorescence typically reached a steady baseline in <10 min, at which point the uncoupler CCCP (2 μM) and respiratory inhibitor antimycin A (2 μM) were introduced, producing an increment in fluorescence intensity that reflects the inherent $\Delta\Psi$ (*31*). Diminished $\Delta\Psi$ levels of experimental samples are expressed as percentages of control levels obtained with nontreated mitochondria.

HPTLC-PI Analysis of Radiolabeled Lipids. Normal-phase high-performance thin-layer chromatography with phosphorimaging radiodetection (HPTLC-PI) was used for monitoring ghost-to-SUV transfer of ^{14}C-labeled Ch, POPC, and overall ChOOH. It was also used for tracking transfer of ^{14}C-labeled Ch, 7α-OOH, and 7α-OH from SUVs to mitochondria. High performance silica gel plates (10 × 20 cm; 0.2 mm layer thickness) from EM Science (Gibbstown, NJ) were used. A dried lipid extract was dissolved in 20 μL of hexane/2-propanol (97:3 v/v) and was applied to the plate in a thin nitrogen stream, using a Linomat IV applicator (Camag Scientific, Wilmington, NC). Separation of Ch from ChOOH or 7α-OOH from 7α-OH was accomplished with benzene/ethyl acetate (1:1 v/v) as the mobile phase. Ch and POPC were separated by a two-step irrigation procedure (*9*). After development, the plate was analyzed for radioactive species

using a Storm 860 storage phosphor system with ImageQuant 4.2 software (Molecular Dynamics, Sunnyvale, CA). Additional details were as described (*7*, *9*, *31*).

HPLC-EC(Hg) Analysis of LOOH Species. High-performance liquid chromatography with mercury cathode electrochemical detection [HPLC-EC(Hg)] was used for monitoring ghost-to-SUV or SUV-to-ghost transfer of individual ChOOH species or PLOOH families. The basic system consists of a model 2350 pump (Isco, Inc., Lincoln, NE) and a model 420 electrochemical detector (EG&G Instruments, Oak Ridge, TN). The detector is equipped with a glass capillary that dispenses a hanging mercury drop, which was set at −150 mV versus a Ag/AgCl reference for the analyses described. Data acquisition and processing was accomplished with EZChrom Elite software (Scientific Software, Inc., Pleasanton, CA). Dried lipid samples were dissolved in 25 μL of 2-propanol, 10 μL being used per chromatographic run. Reverse-phase separation of ChOOHs was carried out at room temperature, using an Ultrasphere XL-ODS column (4.6 × 70 mm; 3 μm particles) from Beckman Instruments (San Ramon, CA) and deoxygenated methanol/acetonitrile/2-propanol/1 mM aqueous sodium perchlorate (80:12:9:10 by vol) as the mobile phase. All ChOOH species except 7α- and 7β-OOH were well-resolved from one another, detection limits being in the 100−200 fmol range. PLOOH separations were carried out using a Supelcosil LC-NH_2 column (4.6 × 150 mm; 3 μm particles) from Supelco (Belleforte, PA) and deoxygenated methanol/2-propanol/40 mM aqueous NaH_2PO_4 (20:10:3 by vol) as the mobile phase. Four major PLOOH families were resolved with this system: PCOOH, PEOOH, PSOOH, and SMOOH, the latter slightly overlapping with PCOOH. Detection limits were in the 0.5−1.0 pmol range. Additional details were as reported (*9*, *15*).

RESULTS

SCP-2-Enhanced Translocation of ChOOH versus Ch. In initial transfer experiments, photoperoxidized egg PC/[^{14}C]-Ch/DCP (5:4:0.1 by mol) SUVs served as donors and unoxidized erythrocyte ghosts as acceptors. The ghosts were in 10-fold lipid molar excess, giving them a large advantage as acceptors. Lipid extracts of SUVs isolated at various times during incubation in the absence or presence of SCP-2 at 37 °C were analyzed for remaining radiolabeled Ch and ChOOH by means of HPTLC-PI. This approach affords an excellent separation of Ch from ChOOHs and other oxidation products; however, individual ChOOH species (positional isomers) are typically not well-resolved from one another (*7*, *8*). Consequently, the transfer behavior of the entire ChOOH population was examined in this phase of the work, the advantage being that this could be compared to parent Ch transfer monitored simultaneously in a common reaction system. Figure 1A shows a representative HPTLC-PI chromatogram depicting the progressive disappearance of Ch and overall ChOOH from SUVs over a 20 min period in the absence [20(−)] or presence (0−20) of bovine liver SPC-2 (75 μg/mL). The starting concentrations of SUV Ch and ChOOH in this experiment were 22.9 and 3.8 μM, respectively (i.e., ∼14% of the original Ch had been converted to ChOOH by photooxidation). Two partially resolved ChOOH bands are seen in Figure 1A, a major one representing 5α-OOH and comigrating 7α/7β-OOH, and a minor one representing

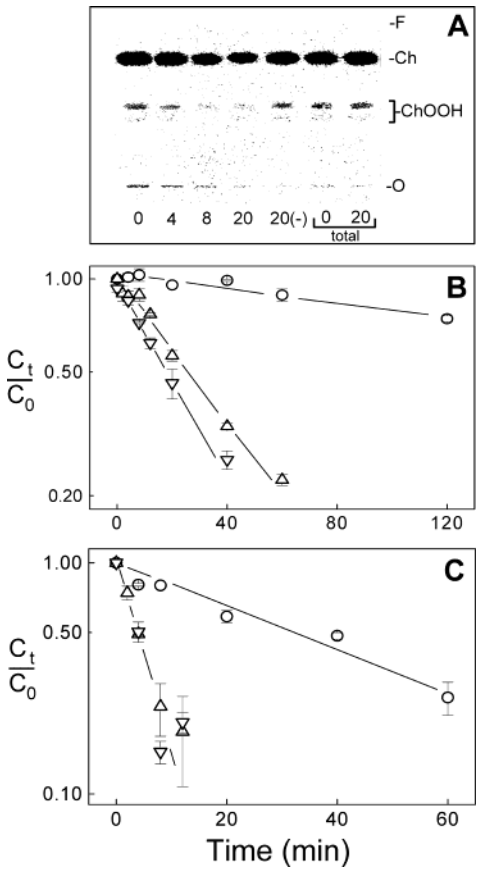

FIGURE 1: SCP-2-enhanced Ch and ChOOH translocation. Reaction mixtures contained photoperoxidized egg PC/[^{14}C]Ch/DCP (5:4:0.1 by mol) SUV donors (0.06 mM total lipid; ∼33 nCi/mL), nonoxidized ghost acceptors (0.6 mM total lipid), 0.52 ± 0.02 unit/mL of bovine liver SCP-2 (75 μg/mL) or human recombinant SCP-2 (25 μg/mL), and BHT (10 μM) in PBS/DFO/EDTA. Mixtures lacking SCP-2 were prepared alongside for determining spontaneous transfer. Starting concentrations of SUV Ch and total ChOOH in bulk suspension were 22.9 and 3.8 μM, respectively. At various time points during transfer incubation at 37 °C, samples were removed, mixed with ice-cold PBS to quench further transfer, and centrifuged. SUV-containing supernatant fractions were extracted, and organic phases were analyzed for remaining Ch and ChOOH by means of HPTLC-PI. (A) HPTLC-PI profiles for bovine SCP-2-mediated transfer at 0, 4, 8, and 20 min. Also shown are a 20 min sample from a system lacking SCP-2 [20(−)] and samples from the total (noncentrifuged) reaction mixture at 0 and 20 min. SUV lipid analyzed: 2.2 nmol per lane (0, 4, 8, 20, 20(−) min); total (SUV + ghost) lipid analyzed: 12.2 nmol per lane (0 and 20 min). The latter samples were scaled down for more accurate measurement of the relative high radioactivity in the Ch band. The upper band in the ChOOH zone represents unresolved 5α-OOH and 7β-OOH, the former predominating; the lower band represents unresolved 6α/6β-OOH and 7α-OOH. (B) First-order kinetic plots for Ch transfer and (C) first-order kinetic plots for ChOOH transfer in the absence (○) or presence of bovine SCP-2 (▽) or human recombinant SCP-2 (△). C_o and C_t denote amount of SUV Ch or ChOOH at time zero and time *t*, respectively. Means ± deviation of values from duplicate experiments are shown, one of which is represented in panel A.

mostly 6α/6β-OOH (*32*). Separate examination by HPLC-EC(Hg) indicated that the initial ChOOH consisted of ∼70% 5α-OOH and 20% 6α/6β-OOH ($^1O_2$ adducts), the remainder being 7α/7β-OOH. Lipid extracts from the entire reaction system (SUVs, ghosts, and aqueous phase) showed that neither the Ch nor the ChOOH band intensity changed over at least a 20 min incubation period. This indicates that no

Table 1: Kinetic Parameters for Spontaneous and Protein-Enhanced Ch and ChOOH Transfer: Comparison of Bovine Liver and Human Recombinant SCP-2[a]

	k (h^{-1})[b]		v ($\mu M\ h^{-1}$)[c]	
protein	Ch	ChOOH	Ch	ChOOH
none	0.15 ± 0.02	1.16 ± 0.14	3.44 ± 0.46	4.40 ± 0.52
bSCP-2	1.53 ± 0.09	7.80 ± 2.70	35.0 ± 2.1	29.6 ± 10.2
hSCP-2	1.38 ± 0.05	8.16 ± 1.14	31.6 ± 1.2	31.0 ± 4.3

[a] Ch and total ChOOH transfer from photoperoxidized SUVs to erythrocyte ghosts was monitored; data are from the experiments described in Figure 1. Protein designations: bSCP-2, bovine liver SCP-2 and hSCP-2, human recombinant SCP-2. [b] Apparent first-order rate constants determined from the decay kinetics of each analyte population in the SUV compartment; values for the SCP-2 systems were not corrected for background (spontaneous) transfer. [c] Initial transfer rates calculated from rate constants and initial concentrations (see Figure 1). Means ± deviation of values from duplicate experiments are shown.

significant further oxidation of Ch or breakdown of ChOOHs with formation of new oxidation products (*31*) occurred under the redox-inhibited transfer conditions used. One can surmise from the results shown in Figure 1A that intermembrane translocation of Ch and ChOOH had occurred and that this was substantially enhanced by SCP-2. No appreciable enhancement was observed when BSA (75 μg/mL) was used instead of SCP-2 (not shown), ruling out the possibility of a nonspecific protein effect. Incubation without ghosts followed by centrifugation revealed no significant loss of SUV signals (not shown), indicating that any aggregation to sedimentable particles was negligible. Semilogarithmic plots depicting the time courses of SUV Ch and ChOOH loss in the absence or presence of SCP-2 are shown in Figure 1B,C; the data are from duplicate experiments, one of which is represented in Figure 1A. Looking first at spontaneous (background) transfer, one sees an apparent first-order decay of Ch (Figure 1B) and ChOOH (Figure 1C), the rate constant for the latter being ~8 times greater (Table 1). Faster spontaneous ChOOH transfer was observed previously (*7*, *8*) using the reverse membrane arrangement (ghost donors and SUV acceptors), but in that case k_{ChOOH} exceeded k_{Ch} by ~65-fold. Whereas k_{ChOOH} was approximately the same for both donors (cf. Table 1, ref *8*), k_{Ch} for ghosts was ~1/8 that for egg PC/Ch/ DCP SUVs, thus accounting for the large difference in k_{ChOOH}/k_{Ch} ratios. Looser lipid packing in the much smaller SUVs (*10*) could have facilitated Ch departure disproportionately over ChOOH departure, thus explaining these findings. The effects of SCP-2 on ChOOH versus Ch transfer were examined, using two different types of protein, bovine liver and human recombinant. As shown in Figure 1B, both proteins at a standardized activity level of 0.52 units/mL stimulated Ch transfer to approximately the same extent. Likewise, ChOOH transfer was accelerated to the same degree (Figure 1C), indicating that the recombinant protein (used in most of the subsequent experiments) was functionally equivalent to a natural counterpart. As shown in Table 1, k_{Ch} was increased ~10-fold and k_{ChOOH} ~7-fold by either SCP-2. However, the net rate constant for facilitated transfer is seen to be ~5.2-fold in favor of ChOOH (6.82 vs 1.31 h^{-1}) (Table 1). Thus, even though the fold enhancement for Ch transfer in the presence of SCP-2 was greater than that for ChOOH, the absolute (background-corrected) rate constant for the latter was substantially higher. Initial rates of SCP-2-mediated Ch and ChOOH transfer (calculated from starting concentrations in SUVs and corrected k values) were found to be similar (i.e., 30.0 and 25.9 μM/h, respectively (Table 1)). Consequently, nearly half of the translocated sterol in the Figure 1 experiment was ChOOH, notwithstanding the fact that its starting concentration was 1/6 that of Ch. SCP-2-stimulated decay of SUV Ch (Figure 1B) leveled off at ~10% remaining sterol after 90 min (not shown). Stimulated decay of ChOOH reached the same level after about 20 min, with no further change thereafter. This suggests that the same equilibrium distribution was reached by both analytes, the ghost acceptor compartment being greatly favored because of its large pool size relative to the SUV compartment.

SCP-2-Facilitated Transfer of Individual ChOOH Species and PLOOH Families. Singlet oxygen-mediated photooxidation of membrane Ch gives rise to three different hydroperoxide species in the following order of abundance: 5α-OOH > 6β-OOH > 6α-OOH (*3*, *17*). Relatively small amounts of 7α- and 7β-OOH are usually also observed, deriving from allylic rearrangement of 5α-OOH or free radical turnover of primary peroxides, including 5α-OOH (3). In follow-up experiments, we reversed the transfer arrangement, using photoperoxidized ghost membranes as donors and SUVs as acceptors. Also, reverse-phase HPLC-EC(Hg) was employed, which allowed different ChOOH positional isomers to be separated and analyzed. As shown in Figure 2A (0 min), peroxidized ghosts contained 7α/7β-OOH, 5α-OOH, 6α-OOH, and 6β-OOH, comprising 19.5, 42.3, 20.8, and 17.4%, respectively, of the total ChOOH in this particular preparation. The overall [ChOOH] was 7.4 μM in bulk suspension, which represents ~6.5% of the starting [Ch]. During a 10 min incubation with DMPC/DCP SUVs in 10-fold lipid excess, there was a progressive decrease in peak area for each ChOOH species, which was markedly enhanced by including recombinant SCP-2 (50 μg/mL) [Figure 2A; compare 10 min with 10 min(−)]. Analysis of the complete system with SCP-2 present (no separation of donor and acceptor membranes) confirmed that there was no significant peroxide loss under the conditions used [Figure 2A; compare 10 min (tot) with 0 min]. First-order plots for spontaneous and SCP-2-stimulated ChOOH transfer from ghost membranes are shown in Figure 2B. A single-exponential decay was observed for each species, an apparent equilibrium being reached with 5−10% of it in the donor compartment (~20 min for 7α/7β-OOH). In agreement with previous findings (*8*, *9*), the rate constants for spontaneous transfer decreased in the following order: 7α/7β-OOH > 5α-OOH > 6α-OOH > 6β-OOH (Table 2), which is identical to the order of decreasing hydrophilicity. Thus, desorption from donor membranes occurred more rapidly as peroxide hydrophilicity increased. As shown in Table 2, SCP-2 increased the rate constants for 6β-OOH, 6α-OOH, 5α-OOH, and 7α/7β-OOH transfer by 1.6-, 2.6-, 4.3-, and 5.6-fold, respectively. Correspondingly, there was a disproportionate increase in the relative rate constants, the 7α/β-OOH value, for example, being 8-fold greater than that of 6β-OOH for spontaneous transfer but 66-fold greater for net SCP-2-facilitated transfer. Transfer kinetics based on peroxide acquisition by SUVs was also determined for the experiment described in Figure 2. Using this approach, we found that the rate constants for net protein-facilitated uptake

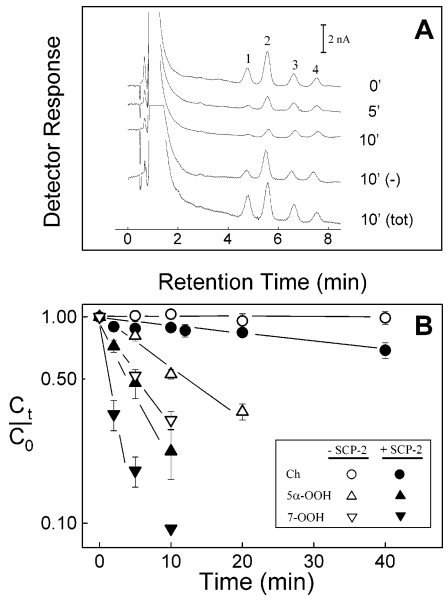

FIGURE 2: SCP-2-enhanced transfer of Ch and ChOOHs from ghost membranes to liposomes. Reaction mixtures contained photooxidized ghosts (0.25 mM total lipid), DMPC/DCP (100:1 by mol) SUVs (2.5 mM total lipid), recombinant SCP-2 [50 μg (1.02 unit)/mL], and 10 μM BHT in PBS/DFO/EDTA. For determining spontaneous transfer, separate mixtures contained everything except SCP-2. Initial concentrations of donor ChOOHs in bulk suspension were as follows: 7α/7β-OOH (1.45 μM), 5α-OOH (3.14 μM), 6α-OOH (1.54 μM), and 6β-OOH (1.29 μM). At various times during incubation at 37 °C, samples were removed, quenched with ice-cold PBS, and centrifuged. Ghost pellets were washed rapidly with cold PBS and extracted. Recovered lipid fractions were analyzed for various ChOOHs by means of HPLC-EC(Hg). Nonperoxidized [^{14}C]Ch-labeled ghosts were used for measuring Ch transfer (see Table 2). (A) Chromatographic profiles showing the progressive loss of ghost ChOOHs in the presence (0−10 min) or absence [10 min (−)] of SCP-2. The entire membrane system with SCP-2 present (ghosts + SUVs) is also represented [10 min (tot)]. Total lipid per injection: 3.8 nmol (ghosts); 10.2 nmol (ghosts + SUVs). Peak assignments: (1) 7α/7β-OOH; (2) 5α-OOH; (3) 6α-OOH; and (4) 6β-OOH. (B) First-order kinetic plots for Ch and ChOOH departure from ghosts in the absence of SCP-2 [Ch (○), 5α-OOH (△), and 7α/7β-OOH (▽)] or presence of SCP-2 [Ch (●), 5α-OOH (▲), and 7α/7β-OOH (▼)]. 6α-OOH and 6β-OOH plots are omitted for clarity. C_o and C_t denote Ch or ChOOH level at time zero and time *t*, respectively. Means ± deviation of values from duplicate experiments are plotted.

of 6β-OOH, 6α-OOH, 5α-OOH, and 7α/ 7β-OOH were 0.21 ± 0.03, 1.12 ± 0.19, 9.63 ± 0.81, and 23.62 ± 6.4 h^{-1} (n = 2), respectively, which compare well with the values based on peroxide departure from ghosts (Table 2). This is consistent with an aqueous transit mechanism of translocation in which desorption from the donor membrane is rate-limiting (*10*). The effects of SCP-2 on Ch transfer kinetics were also examined and compared with those of the ChOOHs. For this, ghost membranes were exchange-loaded with [^{14}C]Ch using SCP-2 but not photoperoxidized before exposing to SUVs; otherwise, the reaction system was identical to that for assessing ChOOH transfer. As shown in Figure 2, Ch spontaneously translocated much more slowly than ChOOHs, the rate constant being ∼90-times lower than that of 7α/7β-OOH, for example (Table 2), which agrees with earlier findings with ghost donors (*8*). Ch transfer from ghosts was significantly slower than from SUVs, as was net SCP-2-stimulated transfer normalized for the same protein concentration (Figures 1 and 2; Tables 1 and 2). Although the fold

Table 2: Rate Constants for SCP-2-Mediated Transfer of Ch, PC, and Various ChOOHs and PLOOHs between Ghost Membranes and Liposomes[a]

	k (h^{-1})[b]		
analyte	−SCP-2	+SCP-2	net
Ch	0.05 ± 0.00	0.49 ± 0.01	0.44 ± 0.03
6β-OOH	0.55 ± 0.05	0.86 ± 0.14	0.31 ± 0.09
6α-OOH	0.83 ± 0.05	2.17 ± 0.20	1.34 ± 0.21
5α-OOH	2.67 ± 0.19	11.60 ± 1.04	8.93 ± 1.36
7α/7β-OOH	4.46 ± 0.65	24.86 ± 2.97	20.40 ± 4.14
POPC	0.03 ± 0.01	0.76 ± 0.15	0.73 ± 0.21
PCOOH	0.35 ± 0.04	2.22 ± 0.25	1.87 ± 0.35
PEOOH	0.40 ± 0.04	2.98 ± 0.39	2.58 ± 0.57
PSOOH	0.46 ± 0.05	2.10 ± 0.18	1.64 ± 0.24

[a] Reaction mixtures for examining protein-facilitated Ch and PC transfer contained [^{14}C]Ch- and [^{14}C]POPC-labeled ghosts [0.25 mM total lipid; ∼30 nCi/mL], DMPC/ DCP (100:1 by mol) SUVs (2.5 mM total lipid), BHT (10 μM), and recombinant SCP-2 (50 μg/mL; ∼1.0 unit/mL) in PBS/DFO/EDTA at 37 °C. Concentrations of ghost Ch and total PC in bulk suspension were ∼110 and ∼42 μM, respectively. Mixtures lacking SCP-2 were prepared alongside for measuring spontaneous transfer. Samples recovered during transfer incubation were centrifuged to separate SUVs from ghosts. The latter were washed and extracted; residual [^{14}C]Ch and [^{14}C]POPC in the lipid fractions were determined by HPTLC-PI. ChOOH and PLOOH data are from the experiments described in Figures 2 and 3, respectively. [b] Apparent first-order rate constants (±SD) for the various analytes represent departure kinetics from ghosts (Figures 2B and 3B). Net rate constants (corrected for spontaneous transfer) are listed in the right column.

increase in transfer rate by SCP-2 was greater for Ch than for any of the ChOOH species, nevertheless all of these species except possibly 6β-OOH had greater net k values (Table 2); for example, the 7α/7β-OOH value was ∼50-times greater than that for Ch. Knowing this and the starting concentrations of ghost membrane Ch and 7α/7β-OOH in the Figure 2 experiment, one finds that the initial rates for net SCP-facilitated Ch and 7α/7β-OOH transfer were 49 and 32 μM/h, respectively. Thus, even though the starting concentration of 7α/7β-OOH was ∼1.3% that of Ch, its initial net rate was only ∼35% lower due to the much higher k value. Similarly, 5α-OOH, the major $^1O_2$ adduct at ∼2.8% the Ch concentration, translocated only ∼40% less rapidly.

As expected, PLOOHs were also generated during photodynamic treatment of ghosts, their overall yield based on total HPLC-EC(Hg)-measurable LOOH, being greater than that of ChOOH (∼87 vs ∼13 mol %). This difference is consistent with the greater molar content of PLs in ghost membranes and the much greater degree of PL unsaturation on average (*20*). Different PLOOH families were determined using recently developed HPLC-EC(Hg) with an amino (LC-NH_2) column (*9*). As shown in Figure 3A, photooxidized ghosts at initial contact with SUVs (0 min) exhibited three well-separated peroxide peaks representing PCOOH, PEOOH, and PSOOH in order of increasing retention time and comprising 43.6, 39.1, and 13.4% of total PLOOH, respectively. Low-yield sphingomyelin hydroperoxide (barely detectable immediately after PCOOH) was not tracked. There was a measurable decrease in each peak area over a 40 min incubation period with SUVs, which was significantly enhanced by SCP-2 [Figure 3A; compare 40 min with 40 min(−)]. No decrease was observed when SUVs were omitted (not shown) or when a sample from the entire reaction mixture was analyzed [Figure 3A, 40(tot)]. Like the ChOOHs, therefore, PLOOHs were stable under the condi-

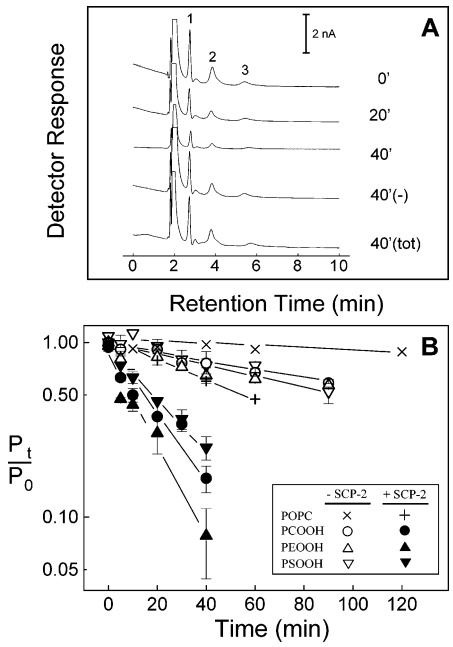

FIGURE 3: SCP-2-enhanced transfer of PC, PCOOH, and various other PLOOHs from ghost membranes to liposomes. Reaction mixtures contained photoperoxidized ghosts (0.25 mM total lipid), DMPC/DCP (100:1 by mol) SUVs (2.5 mM total lipid), BHT (10 μM), and recombinant SCP-2 [50 μg (1.02 unit)/mL, except for spontaneous transfer determination] in PBS/DFO/EDTA at 37 °C. Initial concentrations of donor PLOOHs in bulk suspension were as follows: PCOOH (22.4 μM), PEOOH (20.1 μM), and PSOOH (6.9 μM). Ghost membranes were isolated at various time points during transfer incubation, extracted, and recovered lipid fractions analyzed for PLOOH families by HPLC-EC(Hg). Transfer of unoxidized PC was assessed separately, using [^{14}C]POPC-labeled ghosts (see Table 2). (A) Chromatographic profiles showing the progressive decay of ghost PLOOHs in the presence (0−40 min) or absence [40 min (−)] of SCP-2. The entire membrane system with SCP-2 present is also represented [40 min (tot)]. Total lipid per injection: 3.8 nmol (ghosts) and 10.2 nmol (ghosts + SUVs). Peak assignments are as follows: (1) PCOOH; (2) PEOOH; and (3) PSOOH. The small peak between PCOOH and PEOOH represents peroxidized sphingomyelin, which was not monitored. (B) First-order plots for POPC and PLOOH departure from ghosts in the absence of SCP-2 [POPC (×), PCOOH (○), PEOOH (△), and PSOOH (▽)] or presence of SC-2 [POPC (+), PCOOH (●), PEOOH (▲), and PSOOH (▼)]. P_o and P_t denote POPC or PLOOH level at time zero and time t, respectively. Means values from duplicate experiments are plotted.

tions used. Semilogarithmic plots of residual ghost PLOOH against incubation time are shown in Figure 3B. PCOOH, PEOOH, and PSOOH all exhibited apparent first-order decays with similar rate constants (0.35−0.45 h^{-1}). When SCP-2 was present at the same activity level used for assessing ChOOH and Ch transfer, there was a substantial acceleration of peroxide decay. The kinetics remained apparent first-order, with rate constants elevated by 4.6-, 6.3-, and 7.5-fold for PSOOH, PCOOH, and PEOOH, respectively (Table 2). These amplifications on average were greater than those observed for any of the ChOOH species. Although the net SCP-2-enhanced rate constant for any PLOOH was greater than that of 6α-OOH or 6β-OOH, it was substantially lower than that of 5α-OOH or 7α/7β-OOH (Table 2). Of special note is the fact that the net k values among the PLOOHs differed by no more than ∼60% (Table 2), whereas the corresponding ChOOH values differed by a wide margin (up to nearly 70-fold). This might be explained at least in part by hydrophilicity considerations, the PLOOHs being similar to one another in this regard but the ChOOHs differing substantially. Transfer kinetics of ghost PLOOHs were compared with those of a nonoxidized synthetic PL, exchange-loaded [^{14}C]POPC. Spontaneous POPC transfer was exceedingly slow, the rate constant being <10% that of any PLOOH (Figure 3; Table 2) and <1% that of 7α/7β-OOH, in agreement with previous findings (*9*). SCP-2 at the same activity level used for the other analytes increased the POPC rate constant ∼26-fold, but nevertheless the net k value was lower than that of PCOOH by ∼60% but, surprisingly, higher than that of Ch by ∼65% (Table 2). The latter suggests a slight preference of SCP-2 for PC over Ch, as also reported by others (*33*). From starting concentrations of ghost PLOOHs in the Figure 2 experiment, one calculates the initial rates of net SCP-2-stimulated transfer for PEOOH, PCOOH, and PSOOH as 51.9, 41.9, and 11.3 μM/h, respectively. A relatively low PSOOH level rather than rate constant explains the latter value.

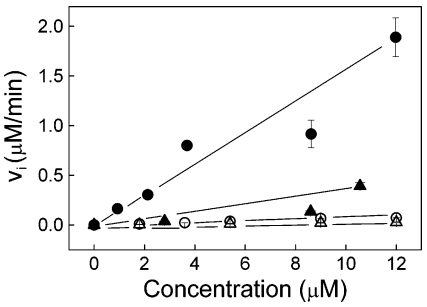

FIGURE 4: Effect of increasing donor substrate concentration on rate of SCP-2-mediated transfer. Four different types of SUV donor were prepared: [^{14}C]Ch/egg PC/DCP, [^{14}C]POPC/egg PC/DCP, 7α-OOH/egg PC/DCP, and POPC-OOH/egg PC/DCP. Transfer of the hydroperoxides and radiolabeled parental lipids was examined. The composition of each SUV type varied as follows (by mol): 1.5:100:1; 3.5:100:1; 6.5:100:1; 16.5:100:1; and 25:100:1. Reaction mixtures contained SUVs (0.06 mM total lipid), ghost acceptors (0.6 mM total lipid), BHT (10 μM), and recombinant SCP-2 [25 μg (0.51 unit)/mL] in PBS/DFO/ EDTA at 37 °C. At various incubation times, transfer was quenched, and SUVs were recovered by centrifugation and extracted. Lipid fractions were analyzed for remaining [^{14}C]Ch (○) or [^{14}C]POPC (△) by scintillation counting and for 7α-OOH (●) or POPC-OOH (▲) by HPLC-EC(Hg) [total lipid per injection: 0.9 nmol (SUVs); 2.4 nmol (SUVs + ghosts)]. Initial concentrations of SUV [^{14}C]Ch, [^{14}C]POPC, 7α-OOH, and POPC-OOH in bulk suspension were 0.9, 2.0, 3.6, 8.4, and 11.9 μM, respectively; radioactivity ranged from 0.05 to 0.50 μCi/mL. Initial rates (v_i) were determined from these concentrations and the corresponding departure rate constants (corrected for spontaneous transfer). Means ± deviation of values from duplicate experiments are plotted.

Transfer Rate in Relation to Substrate or SCP-2 Concentration. Using ghosts as acceptors, we examined SCP-2-enhanced transfer as a function of substrate content of SUV donors. Four different substrates were tracked at a fixed protein level (∼0.5 unit/mL): 7α-OOH, POPC-OOH, [^{14}C]-Ch, and [^{14}C]POPC; each was incorporated into egg PC-based SUVs in increasing proportions from 1.5 to 20 mol %. As shown in Figure 4, net SCP-2-dependent initial transfer rates increased in apparent linear fashion with bulk concentration of each peroxide or parent lipid up to at least 12 μM. Slopes of the 7α-OOH, POPC-OOH, Ch, and POPC plots (equivalent to first-order rate constants) are 8.34, 2.04, 0.46, and 0.14 h^{-1}, respectively. Except for PC versus Ch, this

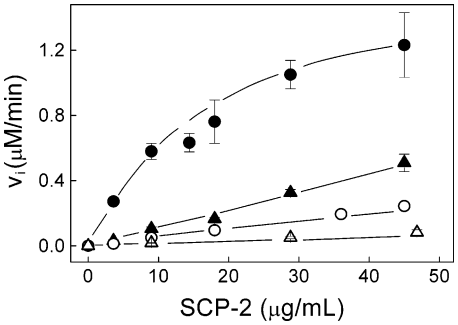

FIGURE 5: Effect of increasing SCP-2 concentration on rate of protein-mediated transfer. Reaction mixtures contained SUV donors (0.15 mM total lipid), ghost acceptors (1.5 mM total lipid), BHT (10 μM), and recombinant SCP-2 in increasing concentrations up to 45 μg/mL (0.9 unit/mL) in PBS/DFO/EDTA at 37° C. SUVs of four different compositions were used: egg PC/Ch/7α-OOH/DCP (50:32:8:0.9 by mol); egg PC/POPC-OOH/Ch/DCP (50:8:32:0.9 by mol); egg PC/[^{14}C]Ch/DCP (50:40:0.9 by mol); and [^{14}C]POPC/Ch/DCP (50:40:0.9 by mol). Radioactivity of [^{14}C]Ch or [^{14}C]POPC was 0.5 μCi/mL. At various time points, SUVs were recovered and analyzed for remaining analyte: 7α-OOH (●) or POPC-OOH (▲) by HPLC-EC(Hg) and [^{14}C]Ch (○) or [^{14}C]POPC (△) by HPTLC-PI. Initial rate (v_i) for each analyte was calculated from its departure rate constant and initial concentration. Mean values from duplicate experiments are plotted.

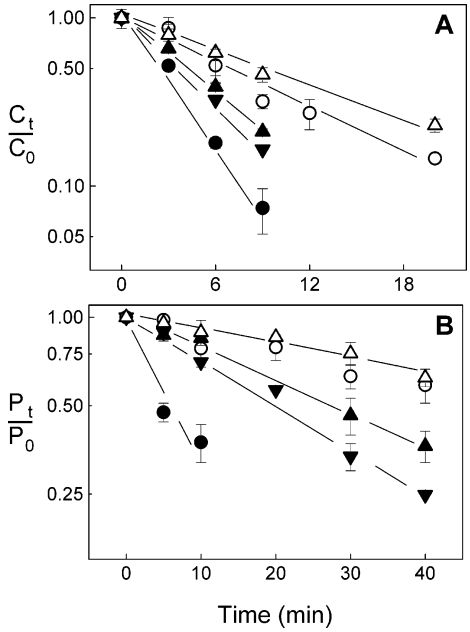

FIGURE 6: Effect of donor phospholipid unsaturation on SCP-2-mediated ChOOH and PLOOH transfer. Increasing SUV unsaturation was imposed by changing the PL component from DMPC to POPC and then to egg PC. PL/Ch/7α-OOH/DCP (50:32:8:1 by mol) SUVs (0.15 mM total lipid) were incubated with ghost acceptors (1.5 mM total lipid) in the absence or presence of recombinant SCP-2 [30 μg (0.61 unit)/mL] in PBS/DFO/EDTA at 37 °C. BHT (10 μM) was included to protect against any possible chain peroxidation. Periodically during incubation, SUVs were isolated by centrifugation and extracted, and recovered lipid fractions were analyzed for remaining 7α-OOH by HPLC-EC(Hg) [total lipid per injection: 2.2 nmol (SUVs); 6.1 nmol (SUVs + ghosts)]. (A) First-order plot for 7α-OOH decay using different PLs in the absence (open symbols) or presence (closed symbols) of SCP-2: DMPC (△, ▲); POPC (▼); and egg PC (○, ●). Transfer of POPC-OOH from PL/POPC-OOH/ Ch/DCP (42:8:40:1 by mol) SUVs was examined in the same way. (B) First-order plot for POPC-OOH decay using different PLs in the absence (open symbols) or presence (closed symbols) of SCP-2: DMPC (△, ▲); POPC (▼); egg PC (○, ●). Means ± deviation of values from duplicate experiments are plotted.

was the same general trend that was observed with ghost membranes as donors (Table 2). Thus, protein-facilitated transfer of the LOOHs was considerably faster than that of the parent lipids, 7α-OOH being most favorable. For all four substrates, including 7α-OOH, there was no indication of an approach to saturation kinetics, at least over the concentration range studied.

Using SUV donors containing ~9 mol % 7α-OOH or POPC-OOH, ~44 mol % [^{14}C]Ch, or ~55 mol % [^{14}C]-POPC, we found that transfer was accelerated with increasing SCP-2 concentration. Kinetic plots were essentially linear up to ~10 μg/ mL for 7α-OOH and up to ~45 μg/mL for POPC-OOH, Ch, or POPC, the initial rate per unit of SCP-2 activity being 3.19, 0.57, 0.27, and 0.09, respectively (Figure 5). These results are consistent with those obtained using ghosts as donors (Figures 2 and 3; Table 2). The flattening observed in the 7α-OOH plot above 28 μg of protein/mL (~2 μM) suggests that peroxide available for transfer was becoming rate-limiting. Using different donor/acceptor systems to study Ch exchange, other investigators have reported that saturation kinetics occurred when [SCP-2] was in the 1−2 μM range (*34*).

LOOH Transfer as a Function of Donor PL Unsaturation. We asked how varying a physical parameter of the donor membrane, viz. degree of PL unsaturation, would affect SCP-2-mediated LOOH transfer. Increasing donor PL unsaturation is known to boost both the spontaneous (*10*) and protein-facilitated (*33*) transfer rate of Ch. To study this for LOOHs, we used saturated DMPC, monounsaturated POPC, and polyunsaturated egg PC SUVs containing 7α-OOH or POPC-OOH as the analyte. There was a small, yet progressive increase in the spontaneous 7α-OOH transfer rate on going from DMPC- to POPC- (not shown) to egg PC-containing SUVs (Figure 6A), suggesting that desorption was favored by increasing PL unsaturation. A similar small effect was apparent for POPC-OOH (Figure 6B). As expected, 7α-OOH transfer was accelerated by SCP-2. The net (background-corrected) rate constants for the DMPC, POPC, and egg PC systems were ~4.8, 6.0, and 10.5 h^{-1}, respectively (Figure 6A), indicating that increasing donor unsaturation also stimulated protein-mediated transfer. POPC-OOH transfer was affected much more dramatically. In this case, the net rate constants for DMPC, POPC, and egg PC SUVs were ~0.8, 1.4, and 6.3 h^{-1}, respectively (Figure 6B). Thus, SCP-2 moved POPC-OOH ~7.8 times faster from egg PC than DMPC SUVs, whereas it moved 7α-OOH only ~2.2 times faster. A possible explanation for this difference is that SCP-2 might bind an LOOH not only on the donor membrane but also in the aqueous compartment. The former mechanism might have been more important for POPC-OOH and the latter for 7α-OOH, which is more hydrophilic.

Transfer Rate as a Function of Donor Negative Charge. SCP-2 has an N-terminal α-helical segment of ~30 amino acids that contains 1/3 of the protein's lysyl residues, displays amphiphilicity, and reportedly serves as a membrane binding domain (*12*, *35*). Previous studies showed that SCP-2-catalyzed Ch transfer is dramatically enhanced by increasing the net negative charge of donor or acceptor membrane with phosphatidylserine (*34*). We adopted a similar approach in

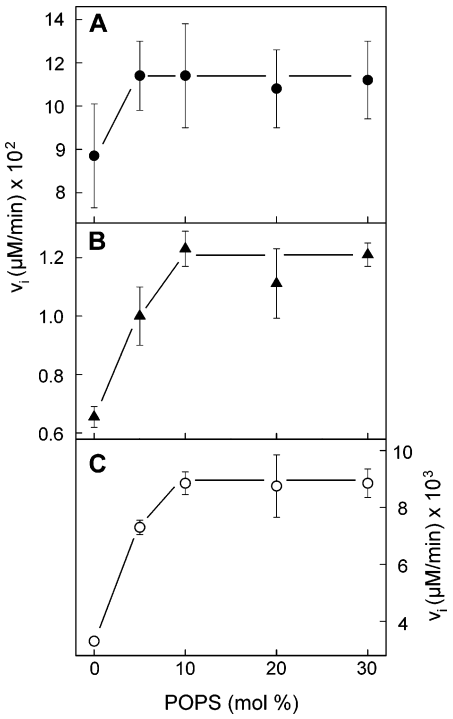

FIGURE 7: Effect of increasing donor negative charge on SCP-2-facilitated transfer of 7α-OOH (A), POPC-OOH (B), and Ch (C). Reaction mixtures at 20 °C contained SUV donors (0.06 mM total lipid), LUV acceptors (0.6 mM total lipid), recombinant SCP-2 (20 μg (0.41 unit)/mL), and BHT (10 μM) in PBS/DFO/EDTA. Different preparations of LacPE/7α-OOH/POPC/POPS SUVs containing 10 mol % each of LacPE and 7α-OOH, increasing amounts of POPS (0, 5, 10, 20, and 30 mol %), and compensatory decreasing amounts of POPC (80, 75, 70, 60, and 50 mol %) were used. POPC/POPS (95:5 by mol) LUVs were used as acceptors. Similar experiments were carried out with LacPE/POPC-OOH/POPC/POPS and LacPE/ [^{14}C]Ch/POPC/POPS SUVs, where replacement of 7α-OOH by POPC-OOH (10 mol %) or [^{14}C]Ch (10 mol %, 0.5 μCi/mL) was the only change. At various incubation times, samples were quenched in ice-cold PBS/DFO/EDTA containing RCA_{120} (0.5 mg/mL). After 10 min, aggregated donor membranes were removed by centrifugation. Recovered acceptor membranes were extracted, and lipid fractions were analyzed for [^{14}C]Ch (○) by scintillation counting or for 7α-OOH (●) or POPC-OOH (▲) by HPLC-EC-(Hg) [total lipid per injection: 0.2 nmol (SUVs) and 2.4 nmol (SUVs + LUVs)]. Initial transfer rates as a function of POPS content are plotted; data points are means from duplicate experiments.

attempting to further characterize SCP-2-mediated LOOH translocation. A SUV donor/ghost acceptor system gave inconsistent results in initial experiments and was replaced with a dual liposome (agglutinable SUV donor/LUV acceptor) system (*28*). In addition to the analyte of interest (10 mol %), donor membranes contained LacPE (10 mol %), POPC (80 → 50 mol %), and POPS (0 → 30 mol %). Agglutination with RCA_{120} under the conditions described consistently resulted in at least 95% recovery of LUVs from SUVs with <2% contamination of the latter. As shown in Figure 7A, the initial rate of SCP-2-catalyzed 7α-OOH transfer increased ~19% upon elevating SUV POPS from 0 to 5 mol %. Further elevation of POPS content up to 30 mol % had no additional effect. By contrast, the rate of protein-catalyzed Ch transfer increased ~180% on going from 0 to 10 mol % POPS and remained constant thereafter up to 30 mol % (Figure 7C). POPC-OOH transfer also accelerated with increasing negative charge density, reaching a maximum of ~85% above background at 10 mol % POPS (Figure 7B). These results are consistent with a model in which electrostatic interactions between positively charged residues near the SCP-2 N-terminus and anionic PL groups on the membrane surface play a key role in protein binding and substrate acquisition (*12*, *34*, *35*). However, the order of responsiveness to increasing membrane negativity (Ch > POPC-OOH > 7α-OOH) qualifies this by suggesting that SCP-2 has an increasing tendency to bind in the aqueous compartment as analyte hydrophilicity goes up (cf. preceding section).

Effect of 7α-OOH Transfer Uptake on Mitochondrial Membrane Potential. SCP-2 plays a key role in Ch trafficking and in adrenocortical cells has been implicated in Ch transport from endoplasmic reticulum to mitochondria for steroid hormone synthesis (*36*). Under oxidative stress conditions, SCP-2-mediated transfer/exchange of ChOOHs and other LOOHs might exacerbate oxidative damage in a target organelle (e.g., mitochondrion). We tested this on a model system consisting of [^{14}C]7α-OOH-bearing SUVs and isolated mouse liver mitochondria. Two parameters were examined: (i) HPTLC-PI-assessed kinetics of spontaneous and SCP-2-stimulated uptake of [^{14}C]7α-OOH by mitochondria and (ii) effect of peroxide acquisition on mitochondrial membrane potential ($\Delta\Psi$), as detected with Rh123. SUVs containing redox-inactive [^{14}C]7α-OH were evaluated similarly. As shown in Figure 8A, 7α-OOH translocated spontaneously to mitochondria, and the rate of uptake was increased significantly by SCP-2 (~1 unit/mL; apparent k ~41.6 vs 10.9 h^{-1}). A sizable reduction of 7α-OOH to 7α-OH and 7β-OH was revealed by HPTLC-PI (~10% at 2 min; ~30% at 5 min), and this was corrected for in the plots. 7α-OOH reduction was negligible when ghost membranes were substituted for mitochondria as acceptors, suggesting that the loss did not occur in transit but rather via one-electron and/or possibly two-electron turnover within the mitochondria (*3*). Flattening of the spontaneous and protein-stimulated uptake curves after 5 min (Figure 8A) is attributed to slower undefined other losses of 7α-OOH, which could not be corrected for. 7α-OH was also taken up by mitochondria, and SCP-2 greatly accelerated this (Figure 8B; apparent k ~13.9 vs 2.3 h^{-1}). Unlike 7α-OOH, 7α-OH accumulated in stable fashion over at least a 10 min period, which accounts for the continuous linearity of the preequilibrium plots in Figure 8B. In the presence of SCP-2 (~1 unit/mL), mitochondria accumulated 7α-OH about one-third as fast as 7α-OOH. Although these uptake rates were not identical, 7α-OH still served as a reasonable control for assessing any redox-related effects of 7α-OOH on membrane potential. Incubation of mitochondria with 7α-OOH-SUVs alone resulted in a slow decrease in $\Delta\Psi$ capacity relative to that of untreated mitochondria, which amounted to ~5% after 10 min (Figure 8C, Table 3) and ~35% after 25 min (not shown). When SCP-2 was included, there was a more dramatic dose- and time-dependent decrease in $\Delta\Psi$ that, at 50 μg of protein/mL, dropped to ~24% of the untreated control level after 10 min (Figure 8C, Table 3). Identical incubation with 7α-OH-SUVs produced only a 15% drop in $\Delta\Psi$, whereas no change was observed when Ch was substituted for 7α-OOH or 7α-OH (Table 3). Supplemental iron in the form of the lipophilic chelate $Fe(HQ)_3$ (2 μM, introduced 5 min before 7α-OOH-SUVs and SCP-2 at 50

Table 3: Comparative Effects of SCP-2-Translocated 7α-OOH, 7α-OH, and Ch on Mitochondrial Membrane Potential[a]

	membrane potential (%)[b]						
	7α-OOH			7α-OH			Ch
SCP-2 (μg/ mL)	2 min	5 min	10 min	2 min	5 min	10 min	10 min
0	100	99	94.5	100	105	99	nd[c]
25	83.5 ± 3.8	69.9	nd	95.9	92.5	nd	nd
50	69.3	66.8 ± 6.9	23.7	85.2 ± 2.1	90.8 ± 4.9	82.1 ± 3.5	104
50[d]	nd	nd	14.8	nd	nd	80.3	nd

[a] Mitochondria (~2.8 mg of protein/mL in MS buffer) were incubated with 7α-OOH- or 7α-OH-containing SUVs in the absence or presence of SCP-2 (25 or 50 μg/mL) for 2, 5, and 10 min (cf. Figure 8). A 10 min incubation with SUVs containing Ch instead of 7α-OOH or 7α-OH was also carried out. Measurements of membrane potential were then performed as described in Figure 8. [b] Membrane potential is represented as a percentage of the control value (no sterol exposure). Where indicated, means ± deviation of values from duplicate determinations are shown. [c] nd, not determined. [d] These mitochondria in MS buffer were treated with 2 μM $Fe(HQ)_3$ for 5 min at 4° C before exposure to 7α-OOH- or 7α-OH-bearing SUVs.

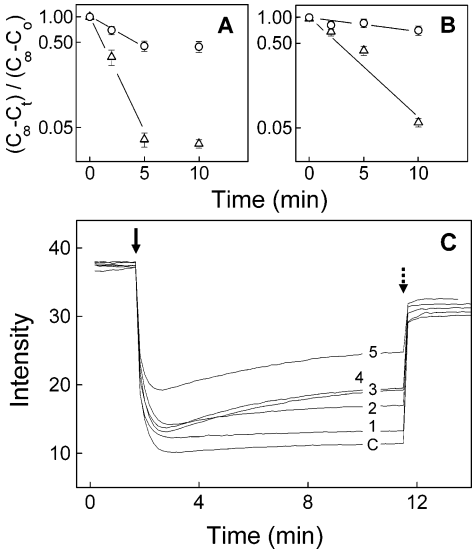

FIGURE 8: SCP-2-enhanced transfer uptake of 7α-OOH or 7α-OH by mitochondria: effects on transmembrane potential. Mouse liver mitochondria (2.84 mg of protein/ mL; ~0.6 mM lipid) were incubated with POPC/[^{14}C]7α-OOH/DCP (80:20:1 by mol) SUVs (0.06 mM lipid; ~25 nCi/mL) in the absence or presence of recombinant SCP-2 (50 μg/mL) in MS buffer at 37 °C. At various times, mitochondria were recovered and extracted, and lipid fractions were analyzed for [^{14}C]7α-OOH and its reduction product [^{14}C]7α-OH by means of HPTLC-PI; lipid load per lane: 22.2 nmol (mito); 12.2 nmol (mito + SUVs). Transfer incubation of mitochondria with POPC/[^{14}C]7α-OH/DCP (80:20:1 by mol) SUVs and subsequent analysis was carried out similarly. (A) First-order kinetic plot for 7α-OOH acquisition in the absence (○) or presence (△) of SCP-2. (B) First-order plot for [^{14}C]7α-OH acquisition in the absence (○) or presence (△) of SCP-2. Mean values from duplicate experiments are plotted in panels A and B. (C) Rh123 fluorescence traces reflecting the effect of transfer-acquired 7α-OOH or 7α-OH on mitochondrial membrane potential. This was examined alongside translocation, using the same incubation conditions, but with nonradiolabeled sterols. In each case, mitochondria were added to ΔΨ assay buffer containing 5 mM sodium succinate, 1 μM rotenone, and 0.2 μM Rh123 at 37 °C, giving 0.2 mg of protein/ mL (solid arrow). After a baseline was attained, 2 μM each of CCCP and antimycin A was introduced (dotted arrow) to deenergize and uncouple the mitochondria, thus allowing ΔΨ to be measured. Tested mitochondrial samples were as follows: (c) control (not treated with SUVs or SCP-2); (1) 10 min with 7α-OOH-SUVs; (2) 10 min with 7α-OH-SUVs + SCP-2; (3) 2 min with 7α-OOH-SUVs +SCP-2; (4) 5 min with 7α-OOH-SUVs + SCP-2; and (5) 10 min with 7α-OOH-SUVs + SCP-2.

μg/mL) exacerbated the loss of ΔΨ, bringing it to 15% of the control level after 10 min (Table 3). On its own, $Fe(HQ)_3$ had no significant effect on ΔΨ, nor did it intensify the small effect observed with 7α-OH-SUVs plus SCP-2 (Table 3). These results are consistent with a mechanism in which iron-catalyzed one-electron reduction of SCP-2-translocated 7α-OOH induced damaging chain peroxidation in mitochondrial membranes, thus impairing ΔΨ generation and other key functions.

DISCUSSION

We have shown that relatively rapid LOOH movement from one membrane to another can be further enhanced by SCP-2, a nonspecific lipid translocator (*11*−*13*, *24*, *25*). This is the first reported evidence for SCP-2 acting in this capacity. When normalized for units of activity, beef liver and human recombinant SCP-2 accelerated ChOOH transfer to the same extent, giving net first-order rate constants for individual species that decreased in the same order as observed for background transfer, viz. 7α/7β-OOH > 5α-OOH > 6α-OOH > 6β-OOH, whereas the background *k* value for the most hydrophilic species, 7α/7β-OOH, was 8 times greater than that for the least hydrophilic, 6β-OOH, and the net *k* with SCP-2 present was nearly 70 times greater. As postulated earlier (*7*, *8*), the rate of peroxide desorption from a donor membrane should increase with increasing polarity, thus producing a larger aqueous transit pool with faster uptake by an acceptor. SCP-2 could further promote transfer by binding and delivering these transit species, although other mechanisms are possible. A kinetic trend similar to the one that we describe for ChOOH isomers has been reported for nonperoxide Ch oxidation products. Thus, initial rates of net SCP-2-enhanced transfer from lipid monolayers to bilayer vesicles increased in the order Ch < 7-ketocholesterol < 7α-hydroxycholesterol < 25-hydroxycholesterol, which is also the order of increasing hydrophilicity of these species (*37*).

Using SUVs as donors, we examined the effects of varying analyte content and protein concentration on SCP-2-facilitated transfer. For 7α-OOH, POPC-OOH, and the corresponding parent lipids, apparent first-order rate constants for net protein-enhanced transfer increased in the following order: POPC < Ch < POPC-OOH < 7α-OOH. A linear relationship was observed between initial transfer rate and increasing peroxide concentration up to 12 μM with no indication of incipient saturation (Figure 4). Saturation may not have been evident because the highest applied molar excess of substrate over SCP-2 was only ~6-fold. Moreover, the large excess of competing SUV lipid (i.e., egg PC) would have limited the amount of SCP-2 available to 7α-OOH, for

example, thus requiring higher competing levels of the peroxide to approach saturation kinetics. However, we were reluctant to exceed 25 mol % (12 μM in bulk) for either peroxide because of possible problems with membrane stability. That SCP-2-facilitated 7α-OOH transfer from SUVs to ghosts showed saturation with respect to protein concentration above ~2 μM (Figure 5) could be explained by either of two factors becoming rate-limiting: availability of hydroperoxide or availability of SCP-2 binding sites on the donor membrane. In contrast, neither POPC-OOH, PC, nor Ch transfer exhibited saturation kinetics over the [SCP-2] range studied. Thus, a maximal desorption rate was reached at a much lower SCP-2 concentration for 7α-OOH than for the other substrates. It is curious that for Ch or dehydroergosterol exchange (*34*), saturation kinetics were observed when SCP-2 reached 1−2 μM, whereas we saw no evidence of this in our system. Differences in vesicle preparation might possibly account for this discrepancy, sonication being used previously (*34*) and extrusion under redox-inhibited conditions being used in this work. Sonication might have unknowingly converted significant amounts of sterol to peroxides and/or other oxides, and this could have biased kinetic measurements to some degree, decreasing the saturation point with SCP-2, for example (cf. Figure 5).

Several possible mechanisms by which SCP-2 facilitates transfer of parent (nonoxidized) lipids have been proposed (*12*, *37*, *38*). One of these suggests that SCP-2 enhances translocation by binding to donor/acceptor membranes and nonspecifically lowering the dissociation/association energy of lipid monomers (*37*). Actual lipid binding by the protein is not necessary according to this model. However, other studies have indicated that SCP-2 has a binding site for Ch (*39*, *40*) as well as PL (*41*) and that alkylation of the cysteine residue in this site with *N*-ethylmaleimide or mersalyl abolishes both binding and transfer activity (*42*). It appears, therefore, that enhanced transfer cannot be explained by SCP-2-membrane interaction alone but that lipid binding by the protein is also necessary. Any of the following mechanisms (*12*) might satisfy these requirements: (i) electrostatic interaction between SCP-2's positively charged N-terminal domain and the negatively charged donor membrane surface, followed by lipid binding, desorption of the protein−lipid complex, and diffusion as such to the acceptor membrane; (ii) formation of a lipid-SCP-2 complex as in (i) but dissociation of the latter after desorption, resulting in faster transfer due to a larger aqueous pool of free lipid; and (iii) transient complex formation in which SCP-2 increases the lipid desorption rate without necessarily leaving the membrane itself. Possibilities (ii) and (iii) are supported by evidence that SCP-2 is still effective when donor and acceptor compartments are separated by a protein-impermeable dialysis membrane (*42*). On the other hand, it has been reported (*34*) that SCP-2-dependent Ch transfer is accelerated with increasing acceptor and donor negative charge, suggesting, as in mechanism (i), that protein interaction with both membrane compartments is necessary for optimal transfer. Since SCP-2 binding of Ch and PL analogues in the absence of membranes has been demonstrated (*39*, *40*), similar binding of spontaneously desorbed lipids might provide an additional pathway for facilitated uptake by acceptor membranes (*12*). This route could be important in the ChOOH and PLOOH transfers that we describe, given that the increased hydrophilicity and faster desorption of these species would make their aqueous pool concentrations significantly greater than those of parental lipids. We postulate that protein-enhanced LOOH transfer occurs via some combination of membrane- and aqueous phase-based binding, the relative importance of the latter increasing with LOOH hydrophilicity. In keeping with this idea is our recent evidence that SCP-2 can bind 5α-OOH under membrane-free conditions (A. Vila and A. W. Girotti, unpublished observation). Additional support derives from the experiments in which donor membrane unsaturation or negative charge density was varied. In agreement with earlier findings based on Ch exchange (*33*, *34*), we found that SCP-2-mediated 7α-OOH and POPC-OOH transfer could be accelerated by increasing the degree of donor PL unsaturation (Figure 6). However, the net rate increments on switching from saturated to monounsaturated to polyunsaturated PL in SUV donors were much greater for POPC-OOH than for 7α-OOH. Of added interest, net Ch transfer under similar reaction conditions (cf. Figure 6) was even more responsive to increasing unsaturation than POPC-OOH transfer (results not shown). Thus, net transfer sensitivity to increasing unsaturation decreased in the following order: Ch > POPC-OOH > 7α-OOH, which is diametrically opposite to the order of decreasing hydrophilicity. Transfer sensitivity to increasing membrane negative charge decreased in the same order for these analytes (Figure 7). Taken together, these results are consistent with the proposed model, viz. mixed on- and off-membrane binding by SCP-2, the latter becoming more important with increasing peroxide hydrophilicity (i.e., concentration in the aqueous compartment).

Using 7α-OOH-bearing SUVs as donors and isolated liver mitochondria as targets, we showed that SCP-2 can exacerbate transfer-dependent peroxide toxicity, as evidenced by the loss of $\Delta\Psi$ (Figure 8). By contrast, Ch- or 7α-OH-containing SUVs had little, if any, effect on $\Delta\Psi$, consistent with 7α-OOH activity being redox related. Like other LOOHs, 7α-OOH is susceptible to iron-catalyzed one-electron reduction, which can trigger membrane-damaging chain peroxidation reactions (*3*, *31*). Such reactions could account for the observed decreases in $\Delta\Psi$. In support of this mechanism was the stimulatory effect of lipophilic iron (Table 3) and the conversion of incoming 7α-OOH to 7α-OH, although two-electron reductive detoxification catalyzed by GPX4 (*3*) might have accounted for some of the latter. GPX4 is the only GSH-dependent selenoenzyme known to detoxify ChOOHs (*3*). In our system, this activity would have been overwhelmed by SCP-2-accelerated peroxide uptake, leading to the observed peroxidative stress damage. The model described has physiological implications in relation to steroidogenesis. For adrenocortical cells, the rate-limiting step in steroid hormone synthesis is Ch translocation from the outer to inner mitochondrial membrane, as mediated by steroidogenic acute regulatory (StAR) protein (*43*). It has been postulated that SCP-2 plays a crucial role in replenishing StAR-depleted outer membrane Ch from various intracellular sources, including plasma membrane and lipid droplets (*36*). Accordingly, if oxidants target the plasma membrane, where Ch is concentrated (*10*), SCP-2 might move ChOOHs adventitiously to mitochondria, thereby disseminating stress damage if detoxification capacity is inadequate. 5α-OOH is of special interest in this regard

because it is reduced more slowly by the GSH/GPX4 system than any other known LOOH (*44*). Other scenarios can be imagined, e.g., LOOH transfer from oxidant-stressed mitochondria to the nucleus, where DNA damage might ensue. We have focused on the cytopathologic potential of LOOH transfer, but there could be beneficial alternatives. For example, movement to subcellular sites where GPX4 or other antioxidants are more abundant might provide a means for more efficient LOOH detoxification (*7*, *8*). Thus, LOOH translocation might have a prooxidant or antioxidant outcome, depending on the circumstances. A question arises as to whether SCP-2-bound LOOHs might be insulated against one-electron turnover that could damage the protein. Although this has not been checked, a recent report indicated that SCP-2 can protect a bound fatty acid analogue against oxidative attack by H_2O_2-derived hydroxyl radical (*45*). Similar sequestration of LOOHs would enhance their lifetimes in transit, thus favoring prooxidant or antioxidant turnover upon delivery.

In summary, we have shown that SCP-2 can promote ChOOH and PLOOH intermembrane transfer with potentially cytotoxic consequences. Whether other lipid transfer proteins (*46*) in cells or plasma can also shuttle these hydroperoxides is presently unknown. Under appropriate conditions, protein-facilitated translocation could greatly expand a LOOH's range of cytotoxic or effector action, a possibility that has not been well-recognized up to now.

ACKNOWLEDGMENT

We thank Fred Schroeder, Barbara Atshaves, and Jeff Billheimer for providing the SCP-2-transformed E. coli strain and for valuable discussions about SCP-2 structure/ function. George Helmkamp's helpful advice regarding agglutinin-based liposome separation is also appreciated. Michele Henry is thanked for making mouse livers available on a regular basis and for helpful suggestions about mitochondria isolation and measurement of membrane potential. This paper is based on research carried out by A.V. in partial fulfillment of the requirements for a Ph.D. degree in Biochemistry at the Medical College of Wisconsin.

REFERENCES

1. Porter, N. A., Caldwell, S. E., and Mills, K. A. (1995) Mechanisms of free radical oxidation of unsaturated lipids, *Lipids 30*, 277−290.
2. Halliwell, B., and Gutteridge, J. M. C. (1990) Role of free radicals and catalytic metal ions in human disease: an overview, *Methods Enzymol. 186*, 1−85.
3. Girotti, A. W. (1998) Lipid hydroperoxide generation, turnover, and effector action in biological systems, *J. Lipid Res. 39*, 1529−1542.
4. Kuhn, H., and Borchert, A. (2002) Regulation of enzymatic lipid peroxidation: the interplay of peroxidizing and peroxide-reducing enzymes, *Free Radic. Biol. Med. 33*, 154−172.
5. Nagata, Y., Yamamoto, Y., and Niki, E. (1996) Reaction of phosphatidylcholine hydroperoxides in human plasma: the role of peroxidase and lecithin: cholesterol acyl transferase, *Arch. Biochem. Biophys. 329*, 24−30.
6. Yamamoto, Y. (2000) Fate of lipid hydroperoxides in blood plasma, *Free Rad. Res. 33*, 795−800.
7. Vila, A., Korytowski, W., and Girotti, A. W. (2000) Dissemination of peroxidative stress via intermembrane transfer of lipid hydroperoxides: model studies with cholesterol hydroperoxides, *Arch. Biochem. Biophys. 380*, 208−218.
8. Vila, A., Korytowski, W., and Girotti, A. W. (2001) Spontaneous intermembrane transfer of cholesterol-derived hydroperoxide species: kinetic studies with model membranes and cells, *Biochemistry 40*, 14715−14726.
9. Vila, A., Korytowski, W., and Girotti, A. W. (2002) Spontaneous transfer of phospholipid and cholesterol hydroperoxides between cell membranes and low-density lipoprotein: assessment of reaction kinetics and prooxidant effects, *Biochemistry 41*, 13705−13716.
10. Phillips, M. C., Johnson, W. J., and Rothblat, G. H. (1987) Mechanisms and consequences of cellular cholesterol exchange and transfer, *Biochim. Biophys. Acta 906*, 223−276.
11. Noland, B. J., Arebalo, R. E., Hansbury, E., and Scallen, T. J. (1980) Purification and properties of sterol carrier protein-2, *J. Biol. Chem. 255*, 4282−4289.
12. Gallegos, A. M., Atshaves, B. P., Storey, S. M., Starodub, O., Petrescu, A. D., Huang, H., McIntosh, A. L., Martin, G. G., Chao, H., Kier, A. B., and Schroeder, F. (2001) Gene structure, intracellular localization, and functional roles of sterol carrier protein-2, *Prog. Lipid Res. 40*, 498−563.
13. Stolowich, N. J., Petrescu, A. D., Huang, H., Martin, G. G., Scott, A. I., and Schroeder, F. (2002) Sterol carrier protein-2: structure reveals function, *Cell. Mol. Life Sci. 59*, 193-212.
14. Lin, F., and Girotti, A. W. (1993) Photodynamic action of merocyanine 540 on leukemia cells: iron-stimulated lipid peroxidation and cell killing, *Arch. Biochem. Biophys. 300*, 714−723.
15. Korytowski, W., Geiger, P. G., and Girotti, A. W. (1999) Lipid hydroperoxide analysis by high-performance liquid chromatography with mercury cathode electrochemical detection, *Methods Enzymol. 300*, 23−33.
16. Korytowski, W., Bachowski, G. J., and Girotti, A. W. (1991) Chromatographic separation and electrochemical determination of cholesterol hydroperoxides generated by photodynamic action, *Anal. Biochem. 197*, 149−156.
17. Girotti, A. W., and Korytowski, W. (2000) Cholesterol as a singlet oxygen detector in biological systems, *Methods Enzymol. 319*, 85−100.
18. Mayer, L. D., Hope, M. J., and Cullis, P. R. (1986) Vesicles of variable size produced by a rapid extrusion procedure, *Biochim. Biophys. Acta 858*, 161−168.
19. Bradford, M. M. (1976) A rapid and sensitive method for the quantitation of microgram quantities of protein utilizing the principle of protein−dye binding, *Anal. Biochem. 72*, 248−254.
20. Ways, P., and Hanahan, D. J. (1964) Characterization and quantification of red cell lipids in normal man, *J. Lipid Res. 5*, 318−328.
21. Holmuhamedov, E. L., Jovanovic, S., Dzeja, P. P., Jovanovic, A., and Terzic, A. (1998) Mitochondrial ATP-sensitive K^+ channels modulate cardiac mitochondrial function, *Am. J. Physiol. 275*, H1567−H1576.
22. Spector, D. L., Goldman, R. D., and Leinwald, L. A. (1998) *Cells: A Laboratory Manual*, Vol. 1, pp 41.2−41.7, Cold Spring Harbor Press, New York.
23. Ardail, D., Privat, J.-P., Egret-Charlier, M., Levrat, C., Lerme, F., and Louisot, P. (1991) Mitochondrial contact sites: lipid composition and dynamics, *J. Biol. Chem. 265*, 18797−18802.
24. Poorthuis, B. J. H. M., Glatz, J. F. C., Akeroyd, R., and Wirtz, K. W. A. (1981) A new high-yield procedure for the purification of the nonspecific phospholipid transfer protein from rat liver, *Biochim. Biophys. Acta 665*, 256−261.
25. Westerman, J., and Wirtz, K. W. A. (1985) The primary structure of the nonspecific lipid transfer protein (sterol carrier protein-2) from bovine liver, *Biochem. Biophys. Res. Commun. 127*, 333−338.
26. Ellman, G. L. (1959) Tissue sulfhydryl groups, *Arch. Biochem. Biophys. 82*, 70−77.
27. Matsuura, J. E., George, H. J., Ramachandran, N., Alvarez, J. G., Strauss, J. F., and Billheimer, J. T. (1993) Expression of the mature and the pro-form of human sterol carrier protein-2 in *Escherichia coli* alters bacterial lipids, *Biochemistry 32*, 567−572.
28. Kasper, A. M., and Helmkamp, G. M., Jr. (1981) Protein-catalyzed phospholipid exchange between gel and liquid crystalline phospholipid vesicles, *Biochemistry 20*, 146−151.
29. Wetterau, J. R., and Zilversmit, D. B. (1984) Quantitation of lipid transfer activity, *Methods Biochem. Anal. 30*, 199−226.
30. Emaus, R. K., Grunwald, R., and Lemasters, J. J. (1986) Rhodamine 123 as a probe of transmembrane potential in isolated rat liver mitochondria: spectral and metabolic properties, *Biochim. Biophys. Acta 850*, 436−448.

31. Korytowski, W., Wrona, M., and Girotti, A. W. (1999) Radiolabeled cholesterol as a reporter for assessing one-electron turnover of lipid hydroperoxides, *Anal. Biochem. 270*, 123−132.
32. Niziolek, M., Korytowski, W., and Girotti, A. W. (2003) Nitric oxide inhibition of free radical-mediated lipid peroxidation in photodynamically treated membranes and cells, *Free Radic. Biol. Med. 34*, 997−1005.
33. Billheimer, J. T., and Gaylor, J. L. (1990) Effect of lipid composition on the transfer of sterols mediated by nonspecific lipid transfer protein (sterol carrier protein-2), *Biochim. Biophys. Acta 1046*, 136−143.
34. Butko, P., Hapala, I., Scallen, T. J., and Schroeder, F. (1990) Acidic phospholipids strikingly potentiate sterol carrier protein-2-mediated intermembrane sterol transfer, *Biochemistry 29*, 4070−4077.
35. Huang, H., Ball, J. M., Billheimer, J. T., and Schroeder, F. (1999) The sterol carrier protein-2 amino terminus: a membrane interaction domain, *Biochemistry 38*, 13231−13243.
36. Gallegos, A. M., Schoer, J. K., Starodub, O., Kier, A. B., Billheimer, J. T., and Schroeder, F. (2000) A potential role for sterol carrier protein-2 in cholesterol transfer to mitochondria, *Chem. Phys. Lipids 105*, 9−29.
37. Van Amerongen, A., Demel, R. A., Westerman, J., and Wirtz, K. W. A. (1989) Transfer of cholesterol and oxysterol derivatives by the nonspecific lipid transfer protein (sterol carrier protein-2): a study of its mode of action, *Biochim. Biophys. Acta 1004*, 36−43.
38. Gadella, T. W. J., Jr., and Wirtz, K. W. A. (1991) The low affinity lipid binding site of the nonspecific lipid transfer protein: implications for its mode of action, *Biochim. Biophys. Acta 1070*, 237−245.
39. Colles, S. M., Woodford, J. K., Moncecchi, D., Myers-Payne, S. C., McLean, L. R., Billheimer, J. T., and Schroeder, F. (1995) Cholesterol interaction with recombinant human sterol carrier protein-2, *Lipids 30*, 795−803.
40. Stolowich, N., Frolov, A., Petrescu, A. D., Scott, A. I., Billheimer, J. T., and Schroeder, F. (1999) Holo-sterol carrier protein-2: ^{13}C NMR investigation of cholesterol and fatty acid binding sites, *J. Biol. Chem. 274*, 35425−35433.
41. Nichols, J. W. (1987) Binding of fluorescent-labeled phosphatidylcholine to rat liver nonspecific lipid transfer protein, *J. Biol. Chem. 262*, 14172−14177.
42. Woodford, J. K., Colles, S. M., Myers-Payne, S. C., Billheimer, J. T., and Schroeder, F. (1995) Sterol carrier portein-2 stimulates intermembrane sterol transfer by direct membrane interaction, *Chem. Phys. Lipids 76*, 73−84.
43. Stocco, D. M. 2000 Intramitochondrial cholesterol transfer, *Biochim. Biophys. Acta 1486*, 184−197.
44. Korytowski, W., Geiger, P. G., and Girotti, A. W. (1996) Enzymatic reducibility in relation to cytotoxicity for various cholesterol hydroperoxides, *Biochemistry 35*, 8670−8679.
45. Dansen, T. B., Kops, G. J. P. L., Denis, S., Jelluma, N., Wanders, R. J. A., Bos, J. J., Burgering, B. M. J., and Wirtz, K. W. A. (2004) Regulation of sterol carrier protein gene expression by the Forkhead transcription factor FOXO3a, *J. Lipid Res. 45*, 81−88.
46. Wirtz, K. W. A. (1997) Phospholipid transfer proteins revisited, *Biochem. J. 324*, 356−360.

BI0491200